Thermal Science and Engineering 2024, 7(3), 8297.
https://doi.org/10.24294/tse.v7i3.8297

Article

Study of different theories of thermoelasticity under the propagation of Rayleigh waves in thermoelastic medium

Manoj Kumar[1], Shruti Goel[1,*], Vandana Gupta[2], Puneet Bansal[3], Pawan Kumar[4]

[1] Baba Mastnath University, Haryana 124021, India
[2] Indira Gandhi National College, Haryana 136132, India
[3] University Institute of Engineering and Technology (UIET), Kurukshetra University, Haryana 136119, India
[4] State Institute of Engineering & Technology (SIET), Kurukshetra University, Haryana 136117, India
*** Corresponding author:** Shruti Goel, shruti1922goel@gmail.com

CITATION

Kumar M, Goel S, Gupta V, et al. Study of different theories of thermoelasticity under the propagation of Rayleigh waves in thermoelastic medium. Thermal Science and Engineering. 2024; 7(3): 8297.
https://doi.org/10.24294/tse.v7i3.8297

ARTICLE INFO

Received: 21 July 2024
Accepted: 24 August 2024
Available online: 10 September 2024

Abstract: The present research is on the propagation of Rayleigh waves in a homogenous thermoelastic solid half-space by considering the compact form of six different theories of thermoelasticity. The medium is subjected to an insulated boundary surface that is free from normal stress, tangential stress, and a temperature gradient normal to the surface. After developing a mathematical model, a dispersion equation is obtained with irrational terms. To apply the algebraic method, this equation must be converted into a rational polynomial equation. From this, only those roots are filtered out, which has satisfied both of the above equations for the propagation of waves decaying with depth. With the help of these roots, different characteristics are computed numerically, like phase velocity, attenuation coefficient, and path of particles. Various particular cases are compared graphically by using phase velocity and attenuation coefficient. The elliptic path of surface particles in Rayleigh wave propagation is also presented for the different theories using physical constants of copper material for different depths and thermal conductivity.

Keywords: coupled model; dual phase lag model; G-N model; three phase lag model; G-L model; L-S model; phase velocity; attenuation coefficient

1. Introduction

The reaction of both natural and artificial materials to wave propagation parameters, such as travel periods (or phase velocities) and wave polarization (particle oscillations), is used to assess the materials. Thermal conductivity, thermal expansion, and specific heat all have an impact on these quantifiable values. The theory of thermoelasticity examines how an elastic medium's temperature affects the way strain and stress are distributed, as well as how induced deformation affects the temperature distribution in the opposite direction.

Biot [1] developed the theory of thermoelasticity known as coupled theory with hyperbolic-parabolic field equations. Green and Lindsay [2] and Lord and Shulman [3] extended the coupled theory and named it generalized thermoelasticity. Green and Naghdi [4] developed a theory of thermoelasticity without energy dissipation. These theories [2–4] admit a finite speed of heat propagation, which creates the difference from coupled theory. Hetnarski and Ignaczak [5] and Ignaczak and Ostoja-Starzewski [6] have reviewed these representative theories of generalized thermoelasticity. Tzou [7] defined the two-stage lag model. Choudhuri [8] identified the initiative in the three-phase lag model. Problems of wave

propagation in coupled or generalized thermoelasticity have been studied by various researchers [9–15].

Wave propagation phenomena have numerous applications in the fields of geophysical exploration, mineral and oil exploration, and seismology. Plane wave propagation in thermoelasticity has many applications in various engineering fields. The surface waves are very helpful for studying various aspects of an earthquake. Rayleigh [16] studied the surface waves that propagate along the free surface of an elastic solid medium. To observe the structural and mechanical properties of any material, these Rayleigh waves are used because waves can travel along the surface and penetrate to a depth of thick solid materials of one wave length and show very sensitive behavior to surface defects. The Rayleigh-type surface waves in thermoelasticity are considered to be used in different engineering fields and future technologies. Many applications of the Rayleigh wave in the theory of thermoelasticity have been reported to date. Some of them are as follows: Lockett [17] studied the effect of a change in Rayleigh wave velocity on a change in thermal conditions. Flavin [18] studied the effect of Rayleigh waves in three mutually perpendicular directions at a constant temperature. Chadwick and Windle [19] studied the effects of the propagation of Rayleigh waves along insulated and isothermal boundaries. Tomita and Shindo [20] examine the effect of magnetic fields on the propagation of Rayleigh waves in a perfectly conducting elastic half-space. Dawn and Chakraborty [21] considered the Rayleigh wave study in thermoelastic media with Green and Lindsay theory. Abd-Alla and Ahmed [22] investigated the influence of initial stress and gravity fields on the propagation of surface waves in an orthotropic thermoelastic medium. Ahmed [23] studied the effect of thermal stress on the propagation of Rayleigh waves in a granular medium. Sharma et al. [24] investigated the effect of Rayleigh surface waves in piezo thermoelastic half-space under the influence of rotation and thermal relaxation. Abouelregal [25] studied the Rayleigh waves in a thermoelastic solid half space using a dual-phase-lag model with surface boundary conditions. Mahmoud [26] investigated the effect of magnetic field, rotation, relaxation times, gravity field, and initial stress on Rayleigh wave velocity in the space of a granular medium. Chirita [27] studied the surface waves in an isotropic thermoelastic half-space. Bucur et al. [28] analyzed the damping effects of thermal fields on Rayleigh waves and plane harmonic waves in a linear thermoelastic material with voids. Passarella et al. [29] considered the G-N theory to study the effect of the propagation of Rayleigh waves in strongly elliptic thermoelastic materials with micro-temperatures.

Biswas et al. [30] considered a three-phase-lag model of thermoelasticity to study the propagation of Rayleigh surface waves in an orthotropic thermoelastic homogenous half-space. Singh and Verma [31] studied the propagation of the Rayleigh wave in thermoelastic solid half-space by considering different theories of thermoelasticity. Kumar and Sangeeta [32] studied the basic equation of thermoelasticity by considering L-S theory under the effects of initial stress, magnetic field, two temperatures, and diffusion. Kumar and Gupta [33] investigated Rayleigh waves in a generalized thermoelastic medium with mass diffusion. Sharma [34,35] studied the Rayleigh wave at the surface of a general anisotropic poroelastic medium: derivation of a real secular equation and Rayleigh waves at the boundary of an

orthotropic elastic solid: influence of initial stress and gravity. Hague and Biswas [36] studied the wave propagation with the help of the Eigen value of an algebraic differential equation. Find phase velocity and attenuation coefficient and compare the graph for void and non-void space. Saeed et al. [37] discussed Rayleigh wave propagation in a semi-conductor thermoelastic medium having temperature-dependent properties.

The present paper is arranged as follows: First, we provide the necessary equations used in the paper and discuss the compact form of the heat conduction equation in Section 2. In Section 3, we formulate the problem in the form of a potential function. In Section 4, find the velocities of longitudinal and transversal waves with the help of potential functions. In Section 5, boundary conditions are applied to find the dispersion equation and its filtered roots. Which are utilized to discover different properties of the Rayleigh wave: the phase velocity, attenuation coefficient, and path of the particle. In Section 6, a comparison between six special cases is exhibited by presenting the phase velocity, attenuation coefficient, and path of the particle traced in motion graphically.

2. Basic equations

Following Kumar and Gupta [38], a compact form of the equations for thermoelasticity theories in the absence of external heat sources are:

The temperature-stress-strain relationship is:

$$\sigma_{ij} = 2\mu e_{ij} + \lambda e_{kk}\delta_{ij} - \delta_{ij}\beta\left(1 + \tau_1\frac{\partial}{\partial t}\right)T \tag{1}$$

Relation between strain and displacement:

$$e_{ij} = \frac{1}{2}(u_{i,j} + u_{j,i}) \tag{2}$$

The equations of motion:

$$(\lambda + \mu)u_{k,ki} + \mu u_{i,kk} - \beta\left(1 + \tau_1\frac{\partial}{\partial t}\right)T_{,i} = \rho\ddot{u}_i \tag{3}$$

Modified Fourier's law:

$$K'\left(n^* + t_1\frac{\partial}{\partial t} + t_3\frac{\partial^2}{\partial t^2}\right)T_{,i} = -q_i \tag{4}$$

Energy equation:

$$\rho T_0\dot{S} = -q_{i,i} \tag{5}$$

Entropy-strain-temperature relation:

$$\rho C_E\left(n_1\frac{\partial}{\partial t} + \tau_0\frac{\partial^2}{\partial t^2} + t_2\frac{\partial^3}{\partial t^3} + t_4\frac{\partial^4}{\partial t^4}\right)T + T_0\beta\left(n_1\frac{\partial}{\partial t} + n_0\tau_0\frac{\partial^2}{\partial t^2} + t_2\frac{\partial^3}{\partial t^3} + t_4\frac{\partial^4}{\partial t^4}\right)e_{kk} = \rho T_0\dot{S} \tag{6}$$

The heat conduction equation:

$$K'\left(n^* + t_1\frac{\partial}{\partial t} + t_3\frac{\partial^2}{\partial t^2}\right)T_{,ii} = \rho C_E\left(n_1\frac{\partial}{\partial t} + \tau_0\frac{\partial^2}{\partial t^2} + t_2\frac{\partial^3}{\partial t^3} + t_4\frac{\partial^4}{\partial t^4}\right)T + T_0\beta\left(n_1\frac{\partial}{\partial t} + n_0\tau_0\frac{\partial^2}{\partial t^2} + t_2\frac{\partial^3}{\partial t^3} + t_4\frac{\partial^4}{\partial t^4}\right)e_{kk}, \tag{7}$$

In the Equations (1)–(7) λ and μ are lame's constants, ρ is the density, C_E is the specific heat at the constant strain, q_i, u_i are heat flux and displacement components,

and increase in temperature. σ_{ij} are stress tensor components, S is entropy per unit mass, $K^{'}$ is thermal conductivity, $T = \theta - T_0$ is small increment in temperature, where T_0 reference temperature and θ absolute temperature with condition satisfied as $|T/T_0| < 1$, e_{kk} is the dilatation, $\beta = (3\lambda + 2\mu)\alpha_t,\ \alpha_t$coefficient of thermal linear expansion, $\tau_0,\ \tau_1,\ \tau_T,\ \tau_q,\ \tau_v$ are thermal relaxation times with condition $\tau_1 \geq \tau_0 \geq 0$, phase lags of temperature gradient, heat flux and thermal displacement gradient respectively, where $n^*,\ n_0,\ n_1, t_1, t_3,\ t_2,\ t_4,\ \tau_0,\ \tau_1,$ are parameters.

Rayleigh wave propagation in a thermoelastic medium. The different theories are studied by using the values of parameters in Equations (3) and (7) as follows:

1) Coupled theory (C-T) condition of thermoelasticity is obtained when.

$$n^* = \mathrm{n}_1 = 1,\ n_0 = t_1 = t_2 = t_3 = t_4 = \tau_0 = \tau_1 = 0 \tag{8}$$

2) The Lord-Shulman (L-S) theory of thermoelasticity is obtained when.

$$n^* = n_0 = n_1 = 1, t_1 = t_2 = t_3 = t_4 = \tau_1 = 0 \tag{9}$$

3) The Green- Lindsay (G-L) theory of thermoelasticity is obtained when.

$$n^* = n_1 = 1,\ n_0 = t_1 = t_2 = t_3 = t_4 = 0 \tag{10}$$

4) The Green-Nagdhi (Type-III) (G-N) theory of thermoelasticity is obtained when.

$$n^* > 0, \mathrm{n}_0 = \tau_0 = t_1 = 1, \mathrm{n}_1 = t_2 = t_3 = t_4 = \tau_1 = 0 \tag{11}$$

Put in Equation (7) results into equation:

$$K^{'}\left(n^* + \frac{\partial}{\partial t}\right) T_{,ii} = \rho C_E \ddot{T} + \beta T_0 \ddot{e}_{kk} \tag{12}$$

Here n^* = constant having a dimension $\frac{1}{sec}$, $\dot{T} = \vartheta$ and $n^* K^{'} = K^{'*}$ is a constant characteristic of the theory. Equation (12) become.

$$K^{'*} T_{,ii} + K^{'} \vartheta_{,ii} = \rho C_E \ddot{T} + \beta T_0 \ddot{e}_{kk} \tag{13}$$

Subcase: When $K^{'} = 0$ in Equation (13) Green-Nagdhi (Type-II) theory is obtained.

5) The two-phase-lag theory of thermoelasticity is obtained when.

$$n^* = 1, n_0 = \ \mathrm{n}_1 = 1, \tau_1 = t_3 = t_4 = 0, t_1 = \tau_T,\ t_2 = \frac{\tau_q^2}{2}, \tau_0 = \tau_q \tag{14}$$

6) The three-phase-lag theory of thermoelasticity is obtained when.

$$n_0 = \tau_0 = 1, n_1 = \tau_1 = 0, t_2 = \tau_q, t_1 = 1 + n^* \tau_v, t_3 = \tau_T, t_4 = \frac{\tau_q^2}{2} \tag{15}$$

3. Formulation of problem

To solve the problem related to two-dimensional space, consider the displacement vector $u = (u_1, 0, u_3)$ in medium. We define the following dimensionless quantities:

$$T^{'} = \frac{\beta T}{\rho c_1^2},\ \left\{x_i^{'}, u_i^{'}\right\} = \left\{\frac{\omega_1^* x_i}{c_1}, \frac{\omega_1^* u_i}{c_1}\right\}\ i = 1, 3,\ \nabla^2 = \frac{\partial^2}{\partial x_1^2} + \frac{\partial^2}{\partial x_3^2},$$
$$t^{'} = \omega_1^* t, \left\{\tau_0^{'}, \tau_1^{'}, \tau_q^{'}, \tau_v^{'}, \tau_T^{'}\right\} = \left\{\tau_0, \tau_1, \tau_q, \tau_v, \tau_T\right\}\omega_1^*, \tag{16}$$
$$\sigma_{ij}^{'} = \frac{\sigma_{ij}}{\beta T_0}, \omega_1^* = \frac{\rho C_E C_1^2}{K^{'}},\ \ C_1^2 = \frac{\lambda + 2\mu}{\rho},\ \ C_2^2 = \frac{\mu}{\rho},\ \delta^2 = \frac{C_2^2}{C_1^2},$$

The displacement components in form of potential function $\phi_1,\ \phi_2,\ \phi_3$can be written as:

$$u_1 = \frac{\partial \phi_1}{\partial x_1} + \frac{\partial \phi_2}{\partial x_1} + \frac{\partial \phi_3}{\partial x_3},\ u_3 = \frac{\partial \phi_1}{\partial x_3} + \frac{\partial \phi_2}{\partial x_3} - \frac{\partial \phi_3}{\partial x_1} \tag{17}$$

In Equations (3) and (7) with the help of (16), after suppressing the primes, apply the Equation (17) we obtain:

$$\left(\nabla^2 - \frac{\partial^2}{\partial t^2}\right)\varphi - \left(1 + \tau_1 \frac{\partial}{\partial t}\right)T = 0 \tag{18}$$

$$\nabla^2 \varphi_3 - \frac{1}{\delta^2}\frac{\partial^2 \varphi_3}{\partial t^2} = 0 \tag{19}$$

$$\left(m^* + t_1 \frac{\partial}{\partial t} + t_3 \frac{\partial^2}{\partial t^2}\right)\nabla^2 T = \left(m_1 \frac{\partial}{\partial t} + \tau_0 \frac{\partial^2}{\partial t^2} + t_2 \frac{\partial^3}{\partial t^3} + t_4 \frac{\partial^4}{\partial t^4}\right)T + \frac{\beta^2 T_0}{\rho^2 C_E c_1^2}\left(n_1 \frac{\partial}{\partial t} + n_0 \tau_0 c \frac{\partial^2}{\partial t^2} + t_2 c^2 \frac{\partial^3}{\partial t^3} + t_4 c^3 \frac{\partial^4}{\partial t^4}\right)\nabla^2 \varphi \tag{20}$$

4. Solution of problem

We assume, for propagation of harmonic wave in consider plane as:

$$\{\phi, \phi_3, T\}(x_1, x_3, t) = \{\bar{\phi}, \bar{\phi}_3, \bar{T}\}e^{-i\omega t} \tag{21}$$

Substitute the Equation (21) in Equations (18) and (20) and then simplified, we get:

$$(Z_1 \nabla^4 + Z_2 \nabla^2 + Z_3)\bar{\varphi} = 0 \tag{22}$$

where:

$$Z_1 = S_2,\ Z_2 = S_2\omega^2 - S_3 - S_1 S_4,\ Z_3 = -\omega^2 S_3\ S_1 = 1 - i\omega\tau_1,\ S_2 = (n^* - it_1\omega - t_3\omega^2)$$

$$S_3 = (-in_1\omega - \tau_0\omega^2 + it_2\omega^3 + t_4\omega^4),$$

$$S_4 = (\beta^2 T_0/\rho^2 C_E C_1^2)(-in_1\omega - \tau_0 n_0\omega^2 + it_2\omega^3 + t_4\omega^4),$$

General solution $\bar{\phi}$ can be written as:

$$\bar{\phi} = \bar{\phi}_1 + \bar{\phi}_2 \tag{23}$$

The potential $\bar{\phi}_1,\ \bar{\phi}_2$ are solutions of equation given by:

$$\left[\nabla^2 + \frac{\omega^2}{V_i^2}\right]\bar{\varphi}_i = 0, \quad i = 1,\ 2 \tag{24}$$

V_1, V_2, are the velocities of longitudinal waves ($P$and SVwave), roots of equation:

$$Z_3 V^4 - Z_2\omega^2 V^2 + Z_1\omega^4 = 0 \tag{25}$$

By using the Equation (21) in Equation (19) we get velocity of transverse wave $V_3 = \delta$ given by:

$$\left[\nabla^2 + \frac{\omega^2}{V_3^2}\right]\bar{\varphi}_3 = 0, \tag{26}$$

By using the Equations (7), (21), (23) and (24) we obtain:

$$\{\varphi, T\} = \sum_{i=1}^{2}\{1, m_i\}\varphi_i, \tag{27}$$

where:

$$m_i = \frac{S_1 S_4 \omega^2}{S_1 S_2 \omega^2 - S_3 {V_i}^2}, \quad i = 1,\ 2$$

The displacement potential ϕ_i for the propagation of harmonic wave with exponential decay in a plane is given as:

$$\varphi_i = A_i e^{i\omega\left(\frac{x_1 + q_i x_3}{c} - t\right)}, \quad i = 1,\ 2,\ 3 \tag{28}$$

where: c is the apparent phase velocity and $q_i = \sqrt{\frac{c^2}{V_i^2} - 1}, \quad i = 1,\ 2, \quad q_3 = \sqrt{\frac{c^2}{\delta^2} - 1}.$

5. Boundary conditions

For the surface which is free from stress and insulated in nature.

Vanish normal and tangential stress component.

$$\sigma_{33} = 0 \tag{29}$$

$$\sigma_{31} = 0 \tag{30}$$

Vanish of temperature gradient normal to insulated surface.

$$\frac{\partial T}{\partial x_3} = 0 \tag{31}$$

By using the Equation (28) in Equations (29)–(31) with the help of Equations (1), (2), (17) and (27) we get system of three homogenous equations as:

$$\sum_{k=1}^{3} c_{ik} A_k = 0 \tag{32}$$

where:

$$c_{11} = -\omega^2 \Pi_1 + 2\frac{\omega^2}{h} - \beta\frac{m_1}{\rho}, \quad c_{12} = -\omega^2 \Pi_2 + 2\frac{\omega^2}{h} - \beta\frac{m_2}{\rho}, \ c_{13} = 2\frac{\omega^2 q_3}{h}, c_{21} = 2q_1, \quad c_{22} = 2q_2, \quad c_{23} = q_3^2 - 1, \quad c_{31} = m_1 q_1, \quad c_{32} = m_2 q_2, \quad c_{33} = 0$$

A non-trivial solution of a homogeneous system of equations is obtained when the determinant of coefficients of Equation (32) vanishes. We get:

$$(2-h)[(2-\Pi_1 h) - \eta(2-\Pi_2 h)(q_1/q_2)] = -4(1-\eta)q_1 q_3 \tag{33}$$

where:

$$h = \frac{c^2}{\delta^2}, \quad \eta = \frac{m_1}{m_2}, \quad \Pi_i = \frac{\lambda + 2\mu}{\rho V_i^2} + \frac{m_i \alpha_t (1 - i\omega\tau_1)}{\omega^2} \quad , i = 1,\ 2$$

In Equation (32) some terms are irrational due to this; it is not possible to solve it by using the algebraic method. To solve this equation, remove radicals by three squaring and manipulation, which reduce the given equation to an algebraic equation of degree 9, written as follows:

$$\sum_{k=0}^{9} c_k h^k = 0 \tag{34}$$

where:

$$c_0 = 2a_0 a_1 - 4(2b_0 b_1 - \varepsilon_s b_0^2)p;$$

$$c_1 = a_1^2 + 2a_0 a_2 - 4\left(b_1^2 + 2b_0 b_2 + \varepsilon_p b_0^2 - 2\varepsilon_s b_0 b_1\right),$$

$$c_2 = 2(a_0 a_3 + a_2 a_1) - 4\left(2b_0 b_3 + 2b_1 b_2 + 2\varepsilon_p b_0 b_1 - \varepsilon_s(b_1^2 + 2b_0 b_2)\right),$$

$$c_3 = a_2^2 + 2a_1 a_3 + 2a_0 a_4 - 4\left[b_2^2 + 2b_1 b_3 + 2b_0 b_4 + \varepsilon_p(b_1^2 + 2b_0 b_2) - 2\varepsilon_s(b_1 b_2 + b_0 b_3)\right],$$

$$c_4 = 2(a_0a_5 + a_1a_4 + a_2a_3) - 4\big[2b_1b_4 + 2b_2b_3 + 2\varepsilon_p b_0b_3 + 2\varepsilon_p b_1b_2 - \varepsilon_s(b_2^2 + 2b_1b_3 + 2b_0b_4)\big],$$

$$c_5 = a_3^2 + 2a_1a_5 + 2a_2a_4 - 4\big[b_3^2 + 2b_2b_4 + \varepsilon_p(b_2^2 + 2b_1b_3 + 2b_0b_4) - 2\varepsilon_s(b_2b_3 + b_1b_4)\big],$$

$$c_6 = 2(a_3a_4 + a_2a_5) - 4\big[2b_3b_4 + 2\varepsilon_p(b_2b_3 + b_1b_4) - \varepsilon_s(2b_2b_4 + b_3^2)\big],$$

$$c_7 = a_4^2 + 2a_3a_5 - 4\big[b_4^2 + \varepsilon_p(2b_2b_4 + b_3^2) - 2\varepsilon_s b_4b_3\big],$$

$$c_8 = 2a_4a_5 - 4\big(2\varepsilon_p b_4b_3 - \varepsilon_s b_4^2\big),\ c_9 = a_5^2 - 4\varepsilon_p b_4^2,$$

$$a_0 = 32\eta,\ a_1 = 16[g_1 + \eta g_2 - \varepsilon_2 - \eta^2\varepsilon_1 + (1-\eta)^2(1+\varepsilon_s)],$$

$$a_2 = 4(g_1^2 + g_2^2) + 8(\Pi_1 + n^2\Pi_2) - 16\big[g_1\varepsilon_2 + ng_2\varepsilon_1 + (1-n)^2\big(\varepsilon_p + \varepsilon_s\big)\big],$$

$$a_3 = 4(\Pi_1 g_1 + \Pi_2 g_2 n - g_1^2\varepsilon_2 - g_2^2\varepsilon_1) - 8(\Pi_1\varepsilon_2 + n\Pi_2\varepsilon_1) + 16(1-n)^2\varepsilon_p,$$

$$a_4 = \Pi_1^2 + n\Pi_2^2 - 4(\varepsilon_2 g_1\Pi_1 + n\varepsilon_1 g_2\Pi_2), a_5 = -(\Pi_1^2\varepsilon_2 + n^2\Pi_2^2\varepsilon_1)$$

$$b_0 = 16\eta,\ b_1 = 8(g_2 + \eta g_1),\ \ b_2 = 4\eta(\Pi_1 + \Pi_2) + 4g_1g_2,$$

$$b_3 = 2(\Pi_1 g_2 + \eta\Pi_2 g_1),\ \ b_4 = \eta\Pi_1\Pi_2,\ g_1 = -(1+\Pi_1),\ \ g_2 = -\eta(1+\Pi_2),$$

$$\varepsilon_s = \varepsilon_1 + \varepsilon_2,\ \varepsilon_p = \varepsilon_1\varepsilon_2,\ \ \varepsilon_i = \left(\frac{\delta}{V_i}\right)^2,\ i = 1,\ 2.$$

An algebraic Equation (34) gives seven complex roots, of which some are added during the removal of radicals. These roots are identified and separated by not satisfying the original dispersion Equation (33). The remaining roots that satisfied Equation (33) are considered for decay of the wave field with an increase of x_3 in the medium. These roots are satisfied, and both the Equations (33) and (34) represent the propagation and existence of Rayleigh waves in an insulated plane boundary of a thermoelastic medium. The coefficient c_i depends upon ω therefore, the phase velocity V calculated from a root of Equation (32) is also a function of ω. This implies the dispersive behavior of the Rayleigh wave on an insulated surface in a thermoelastic medium.

By following Sharma [39], the phase velocity and attenuation coefficient can be calculated as:

Phase Velocity:

$$V = \frac{|c^2|}{Re(c)} = \frac{\delta|h|}{Re(\sqrt{h})} \tag{35}$$

Attenuation Coefficient:

$$Q^{-1} = \frac{Im(1/c^2)}{Re(1/c^2)} = -\frac{Im(h)}{Re(h)} \tag{36}$$

Path of surface Particles:

$$\varphi_i = A_1\gamma_i e^{i(kx_1 - \omega t) + ikx_3 q_i}, i = 1,2,3 \tag{37}$$

where: $\gamma_i = A_i/A_1,\ \ i = 1,2,3$ are solution of Equation (30) and $k = \omega/c$ is the complex number.

where: $\gamma_1 = 1,\ \gamma_2 = -\eta q_1/q_2,\ \ \gamma_3 = 2q_1\left(\frac{\eta-1}{q_3^2-1}\right)$,

By using Equation (37) in Equations (17) and (23), we get:

$$(u_1, u_3) = \big(|U_0|e^{i\arg U_0}, |W_0|e^{i\arg W_0}\big)e^{i(kx_1 - \omega t)} \tag{38}$$

$$\begin{pmatrix} U_0 \\ W_0 \end{pmatrix} = \begin{pmatrix} i\big[\gamma_1 e^{ik_R x_3\delta_1} + \gamma_2 e^{ik_R x_3\delta_2} + \gamma_3 q_3 e^{ik_R x_3\delta_3}\big] \\ \big[\gamma_1 q_1 e^{ik_R x_3\delta_1} + \gamma_2 q_2 e^{ik_R x_3\delta_2} - \gamma_3 e^{ik_R x_3\delta_3}\big] \end{pmatrix} kA_1 e^{i(kx_1 - \omega t)} \tag{39}$$

where: $\delta_i = \left(1 - i\frac{c_I}{c_R}\right) q_i,\ i = 1,\ 2,\ 3.$

R is used for real part and *I* is used for imaginary part of complex quantity, *K* is wave number.

By using Equations (37) and (27), we get:

$$T = |T_0| e^{i\, arg\, T_0} e^{i(kx_1 - \omega t)} \tag{40}$$

$$T_0 = A_1\left(m_1\gamma_1 e^{ik_R x_3 \delta_1} + m_2\gamma_2 e^{ik_R x_3 \delta_2}\right) \tag{41}$$

On the boundary surface $x_3 = 0$ the Equation (38) by considering real part we get:

$$U = |U_0| e^{-k_I x_1} cos(arg\, U_0 + \Phi),\quad W = |W_0| e^{-k_I x_1} \sin(arg\, W_0 + \Phi) \tag{42}$$

$\Phi = K_R x - \omega t$ parameter varies in $(0,2\pi)$ to show the path traced. By using Equations (28) in parametric form traces elliptical path.

Special cases

Case 1: To obtain the secular equation for Coupled theory of thermoelasticity. Put $n^* = \mathrm{n}_1 = 1,\ n_0 = t_1 = t_2 = t_3 = t_4 = \tau_0 = \tau_1 = 0$, in Equation (25).

For $\Pi_1 = 0,\ \eta = 0$ Equation (33) reduces to equation $(2-h)^2 = -4q_1q_3$ which represents Rayleigh wave propagation in elastic medium. Similar to Ewing et al. [40].

Case 2: When the condition $n^* = n_0 = n_1 = 1, t_1 = t_2 = t_3 = t_4 = \tau_1 = 0$, with one relaxation of time, applied in Equation (25), yields the secular equation for L-S theory of thermoelasticity.

Case 3: When the condition $n^* = n_1 = 1,\ n_0 = t_1 = t_2 = t_3 = t_4 = 0$, with two relaxations of times, applied in Equation (25), yields the secular equation for the G-L theory of thermoelasticity.

Case 4: When the condition $n^* > 0, \mathrm{n}_0 = \tau_0 = t_1 = 1, \mathrm{n}_1 = t_2 = t_3 = t_4 = \tau_1 = 0$, applied in Equation (25), we obtained G-N (Type-III) theory of thermoelasticity.

Case 5: To obtain secular equation for Two-phase lag theory of thermoelasticity apply $n^* = 1, n_0 = n_1 = 1, \tau_1 = t_3 = t_4 = 0, t_1 = \tau_T,\ t_2 = \frac{\tau_q^2}{2}, \tau_0 = \tau_q,$ in Equation (25).

Case 6: To obtain secular equation for three-phase lag theory of thermoelasticity apply $n_0 = \tau_0 = 1, n_1 = \tau_1 = 0, t_2 = \tau_q, t_1 = 1 + n^*\tau_v, t_3 = \tau_T, t_4 = \frac{\tau_q^2}{2},$ in Equation (25).

6. Numerical results and discussion

6.1. Findings of phase velocity, attenuation coefficient

The software MATLAB is used to compare phase velocity and attenuation coefficient for the different theories of thermoelasticity by using frequencies in the range of 0.1 Hz to 59.1 Hz.

Now we find numerical results by using physical constants of copper material, followed by [39], which are given below:

$\lambda = 77.6$ GPa, $T_0 = 318$ K, $\alpha_t = 1.78 \times 10^{-5}\mathrm{K}^{-1}$, $\mu = 38.6$ GPa, $\mathrm{C_E} = 383$ J $\mathrm{Kg}^{-1}/\mathrm{K}$, $\rho = 8920$ kg/m^3, $K' = 400\mathrm{Wm}^{-1}$

The relaxation time is given below:

$\tau_0 = 0.1$ s, $\tau_1 = 0.2$ s, $\tau_q = 0.6$ s, $\tau_T = 0.4$ s, $\tau_v = 0.5$ s, $n^* = 0.38710\ \mathrm{sec}^{-1}$.

The output of the program is shown in **Tables 1** and **2** for comparing different theories of thermoelasticity with frequency.

Table 1. Value of phase velocity (V) w.r.t frequency ω in context of different theories of thermoelasticity.

Frequency ω	**C-T (V)**	**L-S (V)**	**G-L (V)**	**G-N (V)**	**DPL (V)**	**TPL (V)**
0.1	0.4923	0.492	0.4908	0.45	0.4917	0.45
1.1	0.437	0.4405	0.4495	0.4544	0.4511	0.4505
2.1	0.4526	0.4596	0.5079	0.4551	0.4985	0.5291
3.1	0.4662	0.4775	0.5152	0.3173	0.3939	0.3975
4.1	0.4765	0.4928	0.4863	0.2416	0.2883	0.3177
5.1	0.4843	0.4742	0.4305	0.1948	0.2211	0.2628
6.1	0.5676	0.4149	0.3712	0.1631	0.1761	0.2233
7.1	0.5267	0.3691	0.3217	0.1403	0.1444	0.1938
8.1	0.4935	0.3324	0.2825	0.1231	0.1212	0.1709
9.1	0.4658	0.3025	0.2514	0.1096	0.1036	0.1528
10.1	0.4423	0.2774	0.2262	0.0988	0.0899	0.1381
11.1	0.422	0.2561	0.2055	0.0899	0.0789	0.126
12.1	0.4043	0.2378	0.1882	0.0825	0.07	0.1158
13.1	0.3887	0.2219	0.1736	0.0762	0.0627	0.1071
14.1	0.3747	0.208	0.1611	0.0708	0.0566	0.0996
15.1	0.3621	0.1957	0.1502	0.0661	0.0514	0.0931
16.1	0.3507	0.1847	0.1407	0.062	0.0469	0.0874
17.1	0.3403	0.1749	0.1323	0.0584	0.0431	0.0823
18.1	0.3308	0.166	0.1249	0.0552	0.0398	0.0778
19.1	0.3221	0.158	0.1182	0.0523	0.0368	0.0738
20.1	0.314	0.1507	0.1123	0.0497	0.0343	0.0701
21.1	0.3065	0.144	0.1068	0.0474	0.032	0.0668
22.1	0.2995	0.1379	0.1019	0.0452	0.0299	0.0638
23.1	0.2929	0.1323	0.0975	0.0433	0.0281	0.0611
24.1	0.2868	0.1271	0.0933	0.0415	0.0264	0.0585
25.1	0.281	0.1223	0.0896	0.0398	0.0249	0.0562
26.1	0.2756	0.1178	0.0861	0.0383	0.0235	0.0541
27.1	0.2705	0.1137	0.0829	0.0369	0.0223	0.0521
28.1	0.2656	0.1098	0.0799	0.0356	0.0212	0.0502
29.1	0.261	0.1062	0.0771	0.0343	0.0201	0.0485
30.1	0.2567	0.1028	0.0745	0.0332	0.0192	0.0469
31.1	0.2525	0.0996	0.0721	0.0321	0.0183	0.0454
32.1	0.2485	0.0966	0.0698	0.0311	0.0174	0.044

Table 1. (*Continued*).

Frequency ω	C-T (V)	L-S (V)	G-L (V)	G-N (V)	DPL (V)	TPL (V)
33.1	0.2448	0.0938	0.0677	0.0302	0.0167	0.0427
34.1	0.2412	0.0911	0.0657	0.0293	0.016	0.0414
35.1	0.2377	0.0886	0.0638	0.0285	0.0153	0.0402
36.1	0.2344	0.0862	0.062	0.0277	0.0147	0.0391
37.1	0.2312	0.084	0.0603	0.0269	0.0141	0.0381
38.1	0.2282	0.0818	0.0587	0.0262	0.0136	0.0371
39.1	0.2252	0.0798	0.0572	0.0256	0.0131	0.0361
40.1	0.2224	0.0778	0.0557	0.0249	0.0126	0.0352
41.1	0.2197	0.076	0.0544	0.0243	0.0122	0.0344
42.1	0.2171	0.0742	0.0531	0.0237	0.0117	0.0336
43.1	0.2145	0.0725	0.0518	0.0232	0.0113	0.0328
44.1	0.2121	0.0709	0.0506	0.0227	0.011	0.032
45.1	0.2097	0.0694	0.0495	0.0222	0.0106	0.0313
46.1	0.2074	0.0679	0.0484	0.0217	0.0103	0.0307
47.1	0.2052	0.0665	0.0474	0.0212	0.01	0.03
48.1	0.2031	0.0651	0.0464	0.0208	0.0097	0.0294
49.1	0.201	0.0638	0.0454	0.0204	0.0094	0.0288
50.1	0.199	0.0626	0.0445	0.02	0.0091	0.0282
51.1	0.197	0.0614	0.0437	0.0196	0.0088	0.0277
52.1	0.1951	0.0602	0.0428	0.0192	0.0086	0.0271
53.1	0.1933	0.0591	0.042	0.0188	0.0084	0.0266
54.1	0.1915	0.058	0.0412	0.0185	0.0081	0.0261
55.1	0.1898	0.057	0.0405	0.0181	0.0079	0.0257
56.1	0.1881	0.056	0.0397	0.0178	0.0077	0.0252
57.1	0.1864	0.055	0.039	0.0175	0.0075	0.0248
58.1	0.1848	0.0541	0.0384	0.0172	0.0073	0.0243
59.1	0.1832	0.0532	0.0377	0.0169	0.0071	0.0239

Table 1 is used to present the findings graphically for comparison of different theories of thermoelasticity. **Figure 1** shows the variation of the phase velocity with respect to frequency for different theories of thermoelasticity. In **Figures 1** and **2**, the solid blue line, red dash line, green dash line with asterisk, red dash line with circle, dark green only asterisk, and sky blue with plus sign correspond respectively to the coupled theory (C-T), Lord-Shulman theory (L-S), Green-Lincoln theory (G-L), Green-Naghdi (Type-III) theory (G-N), two-phase lag theory (DPL), and three-phase lag theory (TPL) of thermoelasticity.

Figure 1 depicts that the phase velocities decrease in all theories smoothly and finally give constant values with an increase in frequency. $\omega = 0.1$ all theories give phase velocity near 0.49 except G-N and three-phase-lag theories, which have little less value in comparison to others. The maximum value of V is attained by coupled theory, and the minimum value is given by two-phase lag theory. Phase velocities given by different Theories follow a pattern: at every fixed value of frequency,

descending values of phase velocity are obtained by theories in the following order: coupled theory, L-S theory, G-L theory, three-phase lag theory, G-N theory, and at the last, two-phase lag theory. In the case of coupled theory, phase velocity takes a curved shape in the range $5.1 \leq \omega \leq 8.1$. Two-phase-lag theory and G-N theory overlap each other in the range $3.1 \leq \omega \leq 6.1$as phase velocities are very close to each other.

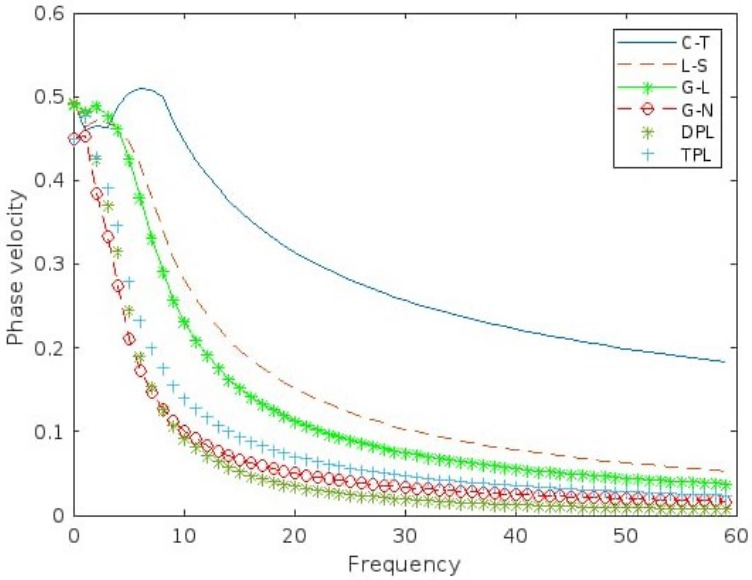

Figure 1. Variation of phase velocities V (m/s) with frequency ω (Hz) for different theories of thermoelasticity.

Table 2 is used to present the findings graphically for comparison of different theories of thermoelasticity. From **Figure 2**, it is depicted that in the case of coupled theory, the value of the attenuation coefficient jumped directly to 6.7789 from −0.1697 and was constant in the range $8.1 \leq \omega \leq 59.1$ up to one decimal place.

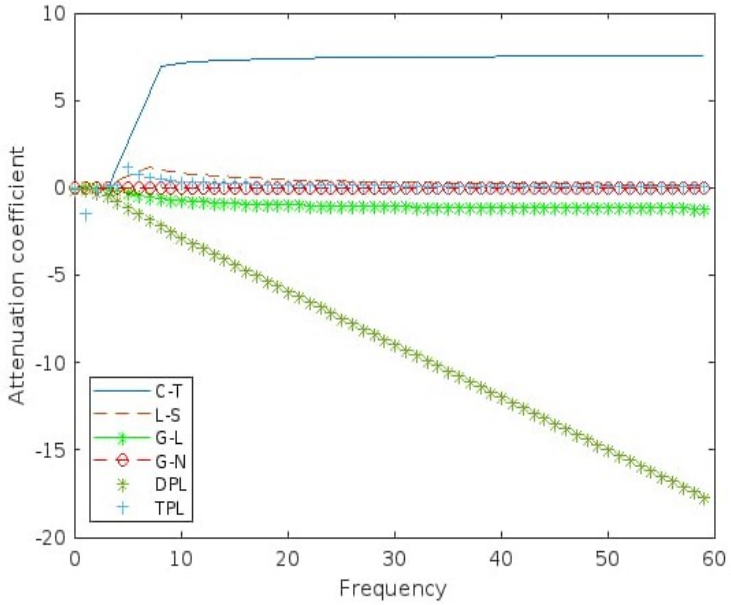

Figure 2. Variation of attenuation coefficient Q^{-1} with frequency ω (Hz) for theories.

Table 2. Value of Attenuation coefficient Q^{-1} w.r.t frequency ω in context of different theories of thermoelasticity.

Frequency ω	**Q^{-1} (C−T)**	**Q^{-1} (L−S)**	**Q^{-1} (G−L)**	**Q^{-1} (G−N)**	**Q^{-1} (DPL)**	**Q^{-1} (TPL)**
0.1	−0.1047	−0.1039	−0.1044	−0.0238	−0.103	0.45
1.1	−0.1101	−0.1071	0.1503	0.0204	−0.0643	0.4505
2.1	−0.1176	−0.1233	0.0975	−0.0719	−0.0053	0.5291
3.1	−0.1386	−0.1563	−0.0444	−0.0479	−0.3867	0.3975
4.1	−0.1562	−0.1916	−0.1856	−0.0379	−0.7994	0.3177
5.1	−0.1697	1.4524	−0.3295	−0.0318	−1.1739	0.2628
6.1	6.7789	1.271	−0.4536	−0.0275	−1.5272	0.2233
7.1	6.9052	1.1323	−0.551	−0.0243	−1.8671	0.1938
8.1	7.0003	1.0217	−0.6278	−0.0217	−2.1979	0.1709
9.1	7.0742	0.931	−0.6897	−0.0197	−2.5224	0.1528
10.1	7.1333	0.855	−0.7407	−0.018	−2.8423	0.1381
11.1	7.1815	0.7904	−0.7834	−0.0166	−3.1588	0.126
12.1	7.2215	0.7348	−0.8199	−0.0154	−3.4726	0.1158
13.1	7.2552	0.6864	−0.8513	−0.0143	−3.7844	0.1071
14.1	7.284	0.6439	−0.8787	−0.0134	−4.0946	0.0996
15.1	7.3087	0.6063	−0.9028	−0.0126	−4.4034	0.0931
16.1	7.3302	0.5728	−0.9241	−0.0119	−4.7112	0.0874
17.1	7.3491	0.5428	−0.9432	−0.0113	−5.018	0.0823
18.1	7.3657	0.5157	−0.9604	−0.0107	−5.3242	0.0778
19.1	7.3804	0.4911	−0.9758	−0.0102	−5.6297	0.0738
20.1	7.3935	0.4688	−0.9899	−0.0098	−5.9346	0.0701
21.1	7.4053	0.4484	−1.0027	−0.0094	−6.2391	0.0668
22.1	7.4159	0.4296	−1.0145	−0.009	−6.5432	0.0638
23.1	7.4255	0.4124	−1.0253	−0.0086	−6.8469	0.0611
24.1	7.4342	0.3965	−1.0352	−0.0083	−7.1503	0.0585
25.1	7.4422	0.3817	−1.0444	−0.008	−7.4535	0.0562
26.1	7.4494	0.368	−1.053	−0.0077	−7.7564	0.0541
27.1	7.4561	0.3552	−1.0609	−0.0074	−8.0591	0.0521
28.1	7.4622	0.3433	−1.0683	−0.0072	−8.3616	0.0502
29.1	7.4679	0.3321	−1.0753	−0.007	−8.664	0.0485
30.1	7.4731	0.3216	−1.0818	−0.0067	−8.9662	0.0469
31.1	7.478	0.3118	−1.0879	−0.0065	−9.2682	0.0454
32.1	7.4825	0.3026	−1.0936	−0.0064	−9.5701	0.044
33.1	7.4867	0.2938	−1.099	−0.0062	−9.8719	0.0427
34.1	7.4906	0.2856	−1.1041	−0.006	−10.1736	0.0414
35.1	7.4943	0.2778	−1.1089	−0.0058	−10.4752	0.0402
36.1	7.4977	0.2704	−1.1135	−0.0057	−10.7767	0.0391
37.1	7.5009	0.2634	−1.1178	−0.0056	−11.0782	0.0381
38.1	7.5039	0.2567	−1.122	−0.0054	−11.3795	0.0371
39.1	7.5068	0.2504	−1.1259	−0.0053	−11.6808	0.0361
40.1	7.5095	0.2444	−1.1296	−0.0052	−11.982	0.0352

Table 2. (*Continued*).

Frequency ω	Q^{-1} (C−T)	Q^{-1} (L−S)	Q^{-1} (G−L)	Q^{-1} (G−N)	Q^{-1} (DPL)	Q^{-1} (TPL)
41.1	7.512	0.2386	−1.1332	−0.005	−12.2832	0.0344
42.1	7.5144	0.2331	−1.1366	−0.0049	−12.5843	0.0336
43.1	7.5167	0.2279	−1.1398	−0.0048	−12.8854	0.0328
44.1	7.5188	0.2229	−1.1429	−0.0047	−13.1864	0.032
45.1	7.5208	0.2181	−1.1459	−0.0046	−13.4873	0.0313
46.1	7.5228	0.2135	−1.1487	−0.0045	−13.7883	0.0307
47.1	7.5246	0.209	−1.1514	−0.0044	−14.0892	0.03
48.1	7.5263	0.2048	−1.154	−0.0044	−14.39	0.0294
49.1	7.528	0.2007	−1.1566	−0.0043	−14.6908	0.0288
50.1	7.5296	0.1968	−1.159	−0.0042	−14.9916	0.0282
51.1	7.5311	0.1931	−1.1613	−0.0041	−15.2923	0.0277
52.1	7.5325	0.1895	−1.1635	−0.004	−15.5931	0.0271
53.1	7.5339	0.186	−1.1657	−0.004	−15.8938	0.0266
54.1	7.5352	0.1826	−1.1678	−0.0039	−16.1944	0.0261
55.1	7.5365	0.1794	−1.1698	−0.0038	−16.4951	0.0257
56.1	7.5377	0.1762	−1.1717	−0.0038	−16.7957	0.0252
57.1	7.5389	0.1732	−1.1736	−0.0037	−17.0963	0.0248
58.1	7.54	0.1703	−1.1754	−0.0036	−17.3969	0.0243
59.1	7.541	0.1674	−1.1771	−0.0036	−17.6974	0.0239

In the case of two-phase lag theory, a straight line is obtained with a decreasing slope as the value of the attenuation coefficient decreases smoothly with an increase in frequency along the negative axis. For the G-L theory, negative values of the attenuation coefficient were obtained with small differences in values and the same for up to one decimal place for increased frequency due to this straight line appearing. The values obtained by L-S and three-phase-lag theories are positive and near to zero within the range of frequency. In the case of the G-N theory, the negative value of the attenuation coefficient obtained very close to zero for increasing values of frequency. Due to the above L-S, G-N, and three-phase-lag theories, they overlap each other.

6.2. Findings of path of particle

All the special cases discussed in the form of different theories of thermoelasticity are presented graphically by using the output of MATLAB software in **Figures 3**–**8**. The polarization of particle motion in two-dimensional space is represented by (U, W).

Physical data of copper material used with frequency $\omega = 2\pi$ and parameter Φ varies in $(0,2\pi)$. Different depths vary as follows: $K_R x_3 = 0,\ 15,\ 45$. The coefficient of thermal linear expansion varies as follows: $\alpha_t = (1.78 \times e^{-2},\ 1.78 \times e^{-3},\ 1.78 \times e^{-4})$ K^{-1}. For one fixed value of depth, we present three figures for three different Coefficient of thermal linear expansion in such a way 9 figures obtained for three different depths in each of **Figures 3**–**8**. Computed for coupled theory, L-S theory, G-L theory, G-N theory, two-phase-lag model, and three-phase-lag model of thermoelasticity.

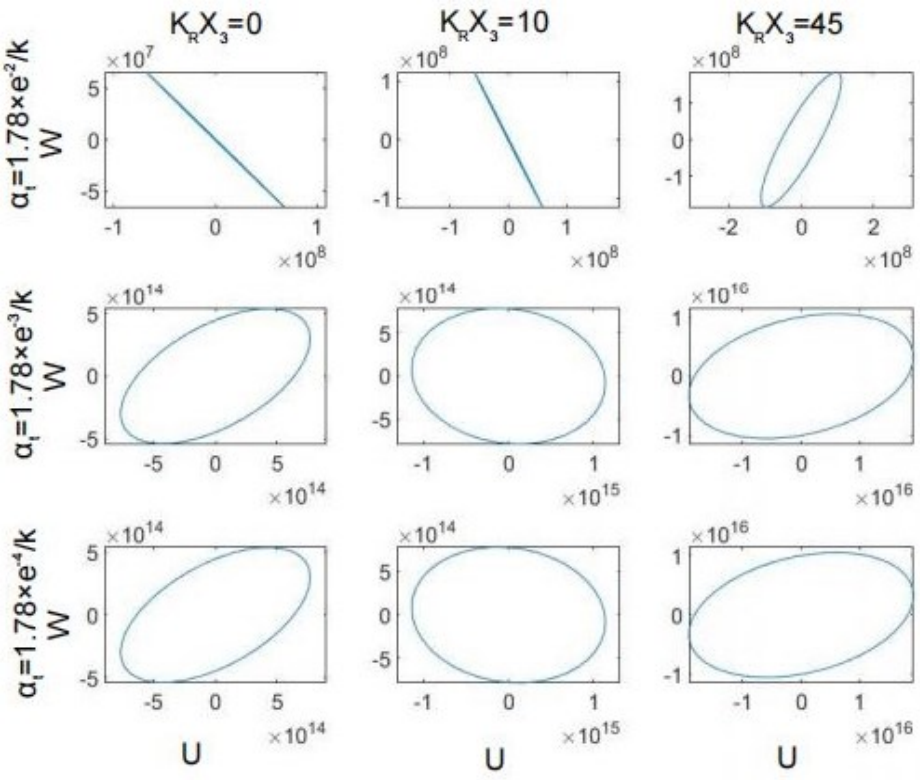

Figure 3. Variation of particle motion (U, W) with depth $K_R x_3 = 0,15,45$ for Couple theory of thermoelasticity and for L-S theory of thermoelasticity respectively.

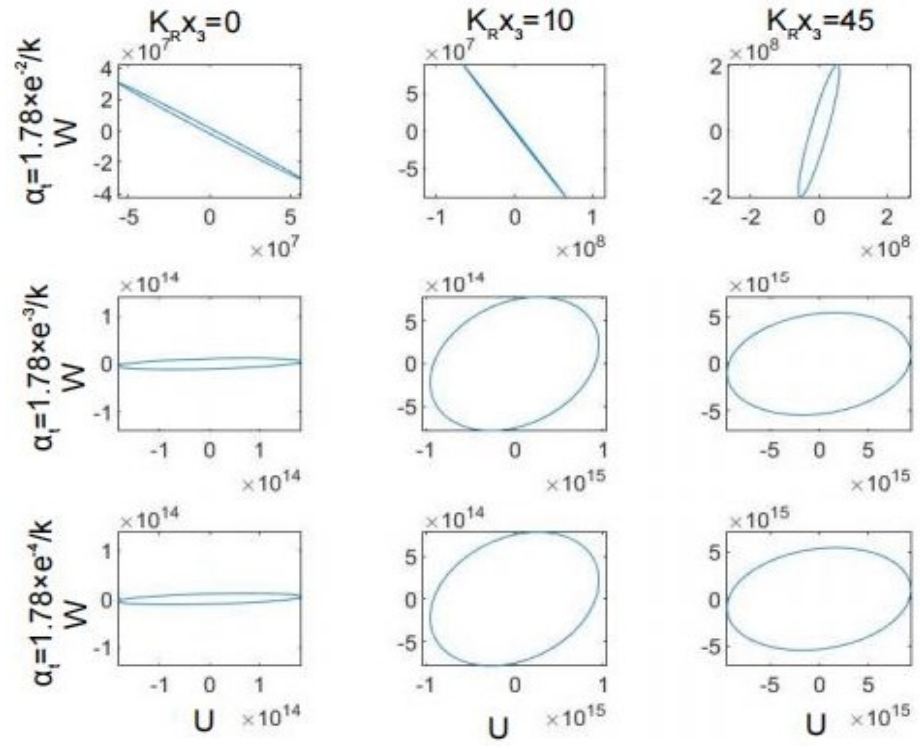

Figure 4. Variation of particle motion (U, W) with depth $K_R x_3 = 0,15,45$ for Couple theory of thermoelasticity and for L-S theory of thermoelasticity respectively.

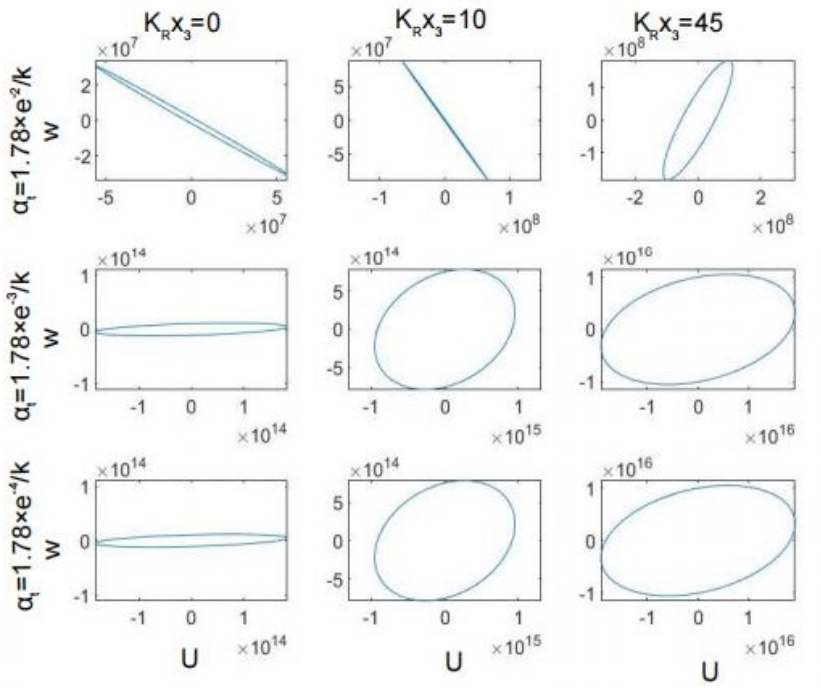

Figure 5. Variation of particle motion (U, W) with depth $K_R x_3 = 0,15,45$ for G-L theory of thermoelasticity and for G-N theory of thermoelasticity.

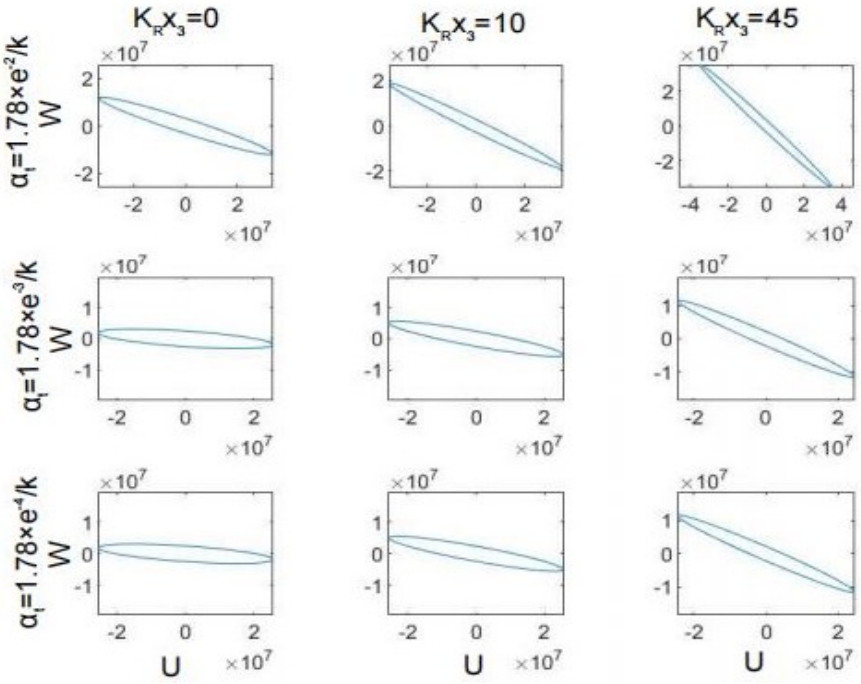

Figure 6. Variation of particle motion (U, W) with depth $K_R x_3 = 0,15,45$ for G-L theory of thermoelasticity and for G-N theory of thermoelasticity.

The effects of α_t on tilted particle motion at different depths are illustrated in **Figures 3**–**8**. It is noted that in the coupled, G-L, and two-phase-lag theories, the amplitude of the Rayleigh wave increases with an increase in values of α_t. The G-N theory shows a constant, and the remaining theories show a decrease in amplitude with an increase in thermal conductivity.

The elliptic path does not change with changes in depth or theories of thermoelasticity. In the case of G-N theory, the amplitude of the Rayleigh wave increases with an increase in the value of depth. The difference in plots of columns is observed as the motion of particle polarization and amplitude are very sensitive to any change in thermal conductivity. Fluctuations are observed in amplitude with depth, as is observed in other theories. Maximum tilt in the case of three-phase-lag theory increases with an increase in depth.

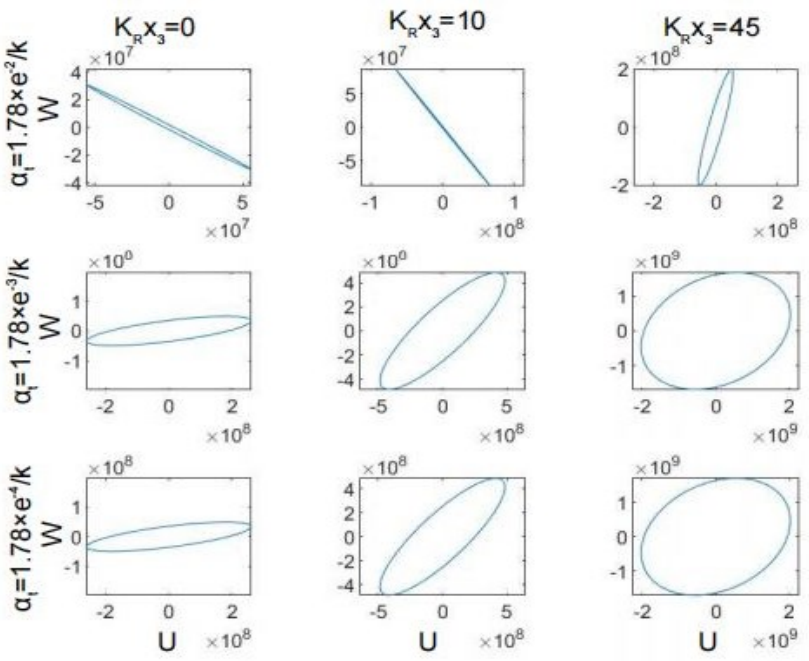

Figure 7. Variation of particle motion (U, W) with depth $K_R x_3 = 0,\ 15,\ 45$ for two phase lag and for three phase lag theory of thermoelasticity.

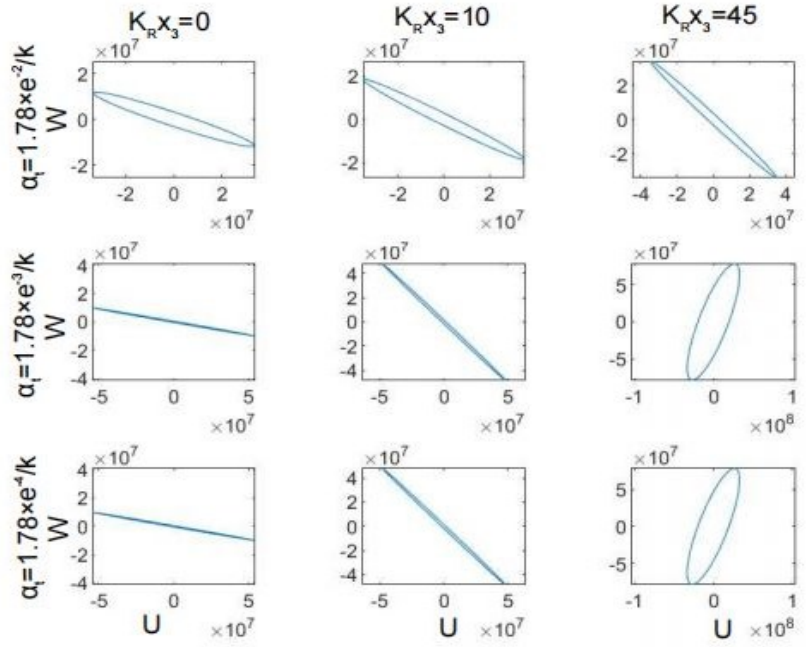

Figure 8. Variation of particle motion (U, W) with depth $K_R x_3 = 0{,}15{,}45$ for two phase lag and for three phase lag theory of thermoelasticity.

7. Conclusion

In this manuscript, the compact form of the heat conduction equation is used to study the coupled L-S, G-L, G-N, two-phase-lag, and three-phase-lag models of thermoelasticity in the propagation of the Rayleigh wave in an isotropic homogenous medium. For insulated surfaces, the dispersion equation is obtained with irrational terms. To obtain a polynomial equation, the dispersion equation is rationalized. Roots are filters that satisfy both equations by checking their decay properties with depth. The comparison of different theories is significant for studying the characteristic properties of the Rayleigh wave.

The phase velocity, attenuation coefficient, and path of particle motion are calculated numerically and presented graphically to compare different theories of thermoelasticity.

The thermally insulated surface reduces the speed of the Ryleigh wave; on the other hand, millions of folds' increases may be noticed in cases of attenuation of the wave.

It is observed that the phase velocity attains its maximum value in the case of coupled theory and its minimum value in the case of two-phase-lag theory. All theories show a smooth, decreasing curve with increasing frequency.

For coupled theory, an instant increase and then constant values of the attenuation coefficient are observed, whereas in the case of two-phase-lag theory, a decreasing slope line is observed with increasing frequency. In the other four theories, values are very close to zero due to this overlapping.

The effect of different theories is significant for the particle motion of the Rayleigh wave and shows an elliptic path for different depths and the coefficient of thermal linear expansion. The Rayleigh wave is one of the surface waves, which is very helpful for studying various aspects of an earthquake.

Author contributions: Conceptualization, MK, VG and SG; methodology, MK, VG and SG ; software, SG, PK and PB; validation, MK, VG and SG; formal analysis, MK, VG, SG, PK and PB; investigation, MK, VG and SG; data curation, MK, VG and SG; writing—original draft preparation, SG; writing—review and editing, MK, VG and SG; supervision, MK and VG. All authors have read and agreed to the published version of the manuscript.

Conflict of interest: The authors declare no conflict of interest.

References

1. Biot MA. Thermoelasticity and Irreversible Thermodynamics. Journal of Applied Physics. 1956; 27(3): 240–253. doi: 10.1063/1.1722351
2. Green AE, Lindsay KA. Thermoelasticity. Journal of Elasticity. 1972; 2(1): 1–7. doi: 10.1007/bf00045689
3. Lord H, Shulman Y. A generalised dynamical theory of thermoelasticity. J. Mech. Phys. Solids. 1967; 15: 299–309. doi: 10.1016/0022-5096(67)90024-5
4. Green AE, Naghdi PM. Thermoelasticity without energy dissipation. Journal of Elasticity. 1993; 31(3): 189–208. doi: 10.1007/bf00044969
5. Richard B, Hetnarski, JI. Generalized Thermoelasticity. Journal of Thermal Stresses. 1999; 22(4–5): 451–476. doi: 10.1080/014957399280832

6. Ignaczak J and Ostoja-Starzewski M. Thermoelasticity with Finite Wave Speeds. Oxford University Press; 2009.
7. Tzou DY. A Unified Field Approach for Heat Conduction from Macro- to Micro-Scales. Journal of Heat Transfer. 1995; 117(1): 8–16. doi: 10.1115/1.2822329
8. Choudhuri SKR. On A Thermoelastic Three-Phase-Lag Model. Journal of Thermal Stresses. 2007; 30(3): 231–238. doi: 10.1080/01495730601130919
9. Deresiewicz H. Effect of boundaries on waves in a thermo-elastic solid: Reflection of plane waves from plane boundary. J. Mech. Phys. Solids. 1960; 8: 164–172. doi: 10.1016/0022-5096(60)90035-1
10. SInha AN, Sinha SB. Reflection of thermoelastic waves at a solid half-space with thermal relaxation. Journal of Physics of the Earth. 1974; 22(2): 237–244. doi: 10.4294/jpe1952.22.237
11. Sinha SB, Elsibai KA. Reflection of Thermoelastic Waves at A Solid Half-Space with Two Relaxation Times. Journal of Thermal Stresses. 1996; 19(8): 749–762. doi: 10.1080/01495739608946205
12. Sharma JN, Kumar V, Chand D. Reflection of generalized thermoelastic waves from the boundary of a half-space. Journal of Thermal Stresses. 2003; 26(10): 925–942. doi: 10.1080/01495730306342
13. Singh MC, Chakraborty N. Reflection of a plane magneto-thermoelastic wave at the boundary of a solid half-space in presence of initial stress. Applied Mathematical Modelling. 2015; 39(5–6): 1409–1421. doi: 10.1016/j.apm.2014.09.013
14. Wei W, Zheng R, Liu G, et al. Reflection and Refraction of P Wave at the Interface Between Thermoelastic and Porous Thermoelastic Medium. Transport in Porous Media. 2016; 113(1): 1–27. doi: 10.1007/s11242-016-0659-1
15. Li Y, Li L, Wei P, et al. Reflection and refraction of thermoelastic waves at an interface of two couple-stress solids based on Lord-Shulman thermoelastic theory. Applied Mathematical Modelling. 2018; 55: 536–550. doi: 10.1016/j.apm.2017.10.040
16. Rayleigh L. On Waves Propagated along the Plane Surface of an Elastic Solid. Proceedings of the London Mathematical Society. 1885; 17(1): 4–11. doi: 10.1112/plms/s1-17.1.4
17. Lockett FJ. Effect of the thermal properties of a solid on the velocity of Rayleigh waves. J. Mech. Phys. Solids. 1958; 7: 71–75. doi: 10.1016/0022-5096(58)90040-1
18. Flavin JN. Thermo-elastic Rayleigh waves in a prestressed medium. Mathematical Proceedings of the Cambridge Philosophical Society. 1962; 58(3): 532–538. doi: 10.1017/s0305004100036811
19. Chadwick P, Windle DW. Propagation of Rayleigh waves along isothermal and insulated boundaries. Royal Society of London Series A Mathematical and Physical Sciences. 1964; 280(1380): 47–71. doi: 10.1098/rspa.1964.0130
20. Tomita S, Shindo Y. Rayleigh waves in magneto-thermoelastic solids with thermal relaxation. Int. J. Eng. Sci. 1979; 17: 227–232. doi: 10.1016/0020-7225(79)90067-3
21. Dawn NC, Chakraborty SK. On Rayleigh wave in Green-Lindsay's model of generalized thermoelastic media. Ind. J. Pure Appl. Math. 1988; 20: 273–286.
22. Abd-Alla AM, Ahmed SM. Rayleigh waves in an orthotropic thermoelastic medium under gravity field and initial stress. Earth, Moon, and Planets. 1996; 75(3): 185–197. doi: 10.1007/bf02592996
23. Ahmed SM. Rayleigh waves in a thermoelastic granular medium under initial stress. International Journal of Mathematics and Mathematical Sciences. 2000; 23(9): 627–637. doi: 10.1155/s0161171200002155
24. Sharma JN, Walia V, K Gupta S. Effect of rotation and thermal relaxation on Rayleigh waves in piezothermoelastic half space. International Journal of Mechanical Sciences. 2008; 50(3): 433–444. doi: 10.1016/j.ijmecsci.2007.10.001
25. Abouelregal AE. Rayleigh waves in a thermoelastic solid half space using dual-phase-lag model. International Journal of Engineering Science. 2011; 49(8): 781–791. doi: 10.1016/j.ijengsci.2011.03.007
26. Mahmoud SR. Influence of rotation and generalized magneto-thermoelastic on Rayleigh waves in a granular medium under effect of initial stress and gravity field. Meccanica. 2012; 47(7): 1561–1579. doi: 10.1007/s11012-011-9535-9
27. Chiriţă S. On the Rayleigh surface waves on an anisotropic homogeneous thermoelastic half space. Acta Mechanica. 2012; 224(3): 657–674. doi: 10.1007/s00707-012-0776-z
28. Bucur AV, Passarella F, Tibullo V. Rayleigh surface waves in the theory of thermoelastic materials with voids. Meccanica. 2013; 49(9): 2069–2078. doi: 10.1007/s11012-013-9850-4
29. Passarella F, Tibullo V, Viccione G. Rayleigh waves in isotropic strongly elliptic thermoelastic materials with microtemperatures. Meccanica. 2016; 52(13): 3033–3041. doi: 10.1007/s11012-016-0591-z
30. Biswas S, Mukhopadhyay B, Shaw S. Rayleigh surface wave propagation in orthotropic thermoelastic solids under three-phase-lag model. Journal of Thermal Stresses. 2017; 40(4): 403–419. doi: 10.1080/01495739.2017.1283971

31. Singh B, Verma S. On Propagation of Rayleigh Type Surface Wave in Five Different Theories of Thermoelasticity. International Journal of Applied Mechanics and Engineering. 2019; 24(3): 661–673. doi: 10.2478/ijame-2019-0041
32. Kumar A, Sangeeta SH. Rayleigh Wave Propagation with The Effect of Initial Stress, Magnetic Field and Two Temperature in The Dual Phase Lag Thermoelasticity. Advances in Mathematics: Scientific Journal. 2020; 9(9): 7535–7545. doi: 10.37418/amsj.9.9.100
33. Kumar R, Gupta V. Rayleigh waves in generalized thermoelastic medium with mass diffusion. Canadian Journal of Physics. 2015; 93(10): 1039–1049. doi: 10.1139/cjp-2014-0681
34. Sharma MD. Rayleigh wave at the surface of a general anisotropic poroelastic medium: derivation of real secular equation. Proceedings of the Royal Society A: Mathematical, Physical and Engineering Sciences. 2018; 474(2211): 20170589. doi: 10.1098/rspa.2017.0589
35. Sharma MD. Propagation of Rayleigh waves at the boundary of an orthotropic elastic solid: Influence of initial stress and gravity. Journal of Vibration and Control. 2020; 26(21–22): 2070–2080. doi: 10.1177/1077546320912069
36. Haque I, Biswas S. Rayleigh waves in nonlocal porous thermoelastic layer with Green-Lindsay model. Steel and Composite Structures. 2024; 50(2): 123-133.
37. Saeed T, Ali Khan M, Alzahrani ARR, et al. Rayleigh wave through half space semiconductor solid with temperature dependent properties. Physica Scripta. 2024; 99(2): 025208. doi: 10.1088/1402-4896/ad17fe
38. Kumar R, Gupta V. Uniqueness, reciprocity theorems and plane wave propagation in different theories of thermoelasticy. International Journal of Applied Mechanics and Engineering. 2013; 18(4): 1067–1086. doi: 10.2478/ijame-2013-0067
39. Sharma MD. Propagation and attenuation of Rayleigh waves in generalized thermoelastic media. Journal of Seismology. 2013; 18(1): 61–79. doi: 10.1007/s10950-013-9401-4
40. Ewing WM, Jardetzky WS, Press F, et al. Elastic Waves in Layered Media. Physics Today. 1957; 10(12): 27–28. doi: 10.1063/1.3060203